Promising ZT values in Ge-doped In_2O_3 n-type thermoelectric oxide

D. Bérardan, E. Guilmeau, A. Maignan, B. Raveau

Laboratoire CRISMAT, UMR 6508 CNRS-ENSICAEN, 6 Boulevard du Maréchal Juin,
14050 CAEN Cedex, France
Contact author: emmanuel.guilmeau@ensicaen.fr, david.berardan@u-psud.fr

ABSTRACT

We have studied the chemical, structural and transport properties of a series of In_2O_3 based samples with germanium doping (from 0 to 15 atom%). X-ray diffraction and scanning electron microscopy studies show that the solubility limit of Ge in In_2O_3 is very small and that additions of more than about 0.5 atom% Ge lead to the presence of $In_2Ge_2O_7$ inclusions. The electrical conductivity is strongly enhanced by Ge doping with best values exceeding 1200 $S.cm^{-1}$ at room temperature. On the other hand, the thermopower decreases with Ge addition, but the thermoelectric power factor remains higher than that of undoped In_2O_3 and is close to 1 $mW.m^{-1}.K^{-2}$ at 1100K in $In_{1.985}Ge_{0.015}O_3$. We show that the evolution of the electrical resistivity and of the thermopower with germanium substitution is directly linked to the evolution of the electrons concentration. The thermal conductivity is strongly reduced by Ge additions. The dimensionless figure of merit ZT reaches 0.1 at 1273K in In_2O_3 and exceeds 0.45 at 1273K in composite compounds with nominal composition $In_{2-x}Ge_xO_3$.

INTRODUCTION

In the past decade, a great effort of research has been devoted to the development of novel materials for applications in thermoelectric energy conversion (see for example ref. 1). Thermoelectric generation systems can directly convert heat energy into electrical power without moving parts or carbon dioxide production. The efficiency of a thermoelectric material used for power generation increases with the so-called dimensionless figure of merit ZT defined as $ZT = S^2T\sigma/\lambda$, where S is the Seebeck coefficient or thermopower, σ the electrical conductivity, and λ the thermal conductivity. The thermal conductivity can be divided into two parts, the first one λ_L originating from the heat carrying phonons, and the second one λ_{elec} which is linked to the electrical conductivity by the Wiedmann-Franz law (valid for metallic-like conductivity) $\lambda_{elec}=L_0T\sigma$ with L_0 the Lorentz number $2.45.10^{-8}$ $V^2.K^{-2}$. Compared with conventional thermoelectric materials, which are mainly intermetallic compounds (see for example ref. 2), oxides are very suitable for high temperature applications due to their high chemical stability under air. Several families of n-type oxide materials have been studied up to now, but all of them exhibit rather poor thermoelectric performances even in single crystals, with best ZT values hardly exceeding 0.3-0.35 at 900-1000°C [3-5] in Al-doped ZnO or textured $(ZnO)_mIn_2O_3$. These ZT values are quite small as compared to those of intermetallic materials like for example $Mg_2Si_{(1-x)}Sn_x$ or skutterudites, but these materials have to be coated to keep their transport properties unchanged when used in air at high temperature. In this contribution, we show that In_2O_3 based compounds, which are known to exhibit very good electrical conductivity and are widely used as transparent conducting oxides (TCO) (see for example ref. 6), exhibit very promising thermoelectric properties making them suitable for applications in high temperature energy conversion modules.

EXPERIMENTAL

All samples, belonging to the $In_{2-x}Ge_xO_3$ series, were prepared using a standard solid reaction route as described in ref. 7.

X-ray powder diffraction (XRD) was employed for structural characterization using a Philips X'Pert Pro diffractometer with X'Celerator using Cu-K$_\alpha$ radiation in a 2θ range 10°-90°. The XRD patterns were analyzed using the Rietveld method with the help of the FullProf software [8].

The scanning electron microscopy (SEM) observations were made using a FEG Zeiss Supra 55. The cationic compositions were determined by energy dispersive X-ray spectroscopy (EDX) EDAX.

The electrical conductivity and thermopower were measured simultaneously using a ULVAC-ZEM3 device between 50°C and 800°C under helium. The thermal conductivity was obtained at 26°C, 300°C, 800°C and 1000°C from the product of the geometrical density, the heat capacity (Netzsch model DSC 404C Pegasus) and the thermal diffusivity (Netzsch model 457 MicroFlash laser flash apparatus). The Hall effect measurements were performed using a commercial quantum design PPMS at 300K between -7 and +7 teslas. The Hall coefficient was deduced from the slope of the Hall resistivity versus field curves, $\rho_H(H)$. The electrons concentration was calculated from the Hall coefficient R_H assuming a single-carrier model and a Hall factor of unity.

RESULTS AND DISCUSSION

The thermal treatment presented above leads to well crystallized samples. Figure 1 shows the Rietveld refinement of a sample with nominal composition $In_{1.9}Ge_{0.1}O_3$. All Bragg peaks can be indexed taking into account a mixture of In_2O_3 (S.G. Ia-3 ref. 9) as main phase and $In_2Ge_2O_7$ (S.G. C2/m ref. 10) as secondary phase. No systematic evolution of the lattice parameter a occurs when the germanium fraction increases despite the very different ionic radii of

In(+III) and Ge(+IV) [11], and the fractions of $In_2Ge_2O_7$ determined using Rietveld refinement of the X-ray diffraction patterns are very close to those expected without substitution (see inset of figure 1). Therefore, either Ge does not substitute in In_2O_3 or the solubility limit is very small.
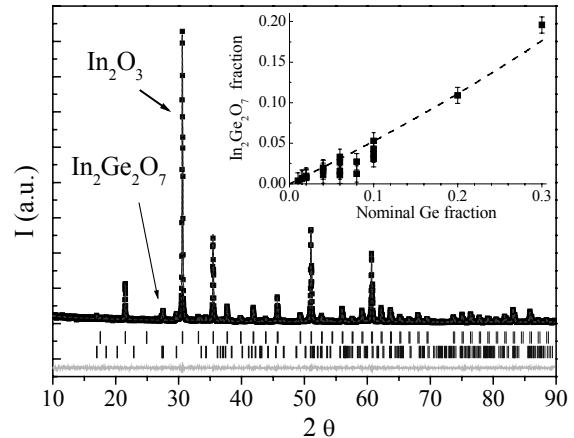

Figure 1: XRD pattern and Rietveld refinement for a sample with nominal composition $In_{1.9}Ge_{0.1}O_3$. Inset: $In_2Ge_2O_7$ fraction determined from Rietveld refinement as a function of the nominal germanium fraction. The dashed curve corresponds to the theoretical $In_2Ge_2O_7$ fraction assuming that no substitution occurs.

This result is confirmed by SEM observations coupled to EDX analyses (Figure 2), which show the presence of $In_2Ge_2O_7$ inclusions as a secondary phase (dark grains) and which do not allow to evidence the presence of germanium in the main phase within the detection limit of EDX spectroscopy. As can be seen in the SEM image, part of the $In_2Ge_2O_7$ inclusions form sphere-like agglomerates inducing some porosity. Therefore, the presence of $In_2Ge_2O_7$ inclusions has a negative effect on the samples densification: the geometrical density strongly decreases from 91% with x=0 to 82% with x=0.2 and 74% with x=0.3. This effect on the densification probably originates from both the formation of the agglomerates, which might be linked to the ball-milling process that does not lead to a good mixing of the precursors, and from a decrease of the grain boundaries mobility that prevents a good filling of the initial porosity of the green pellets.
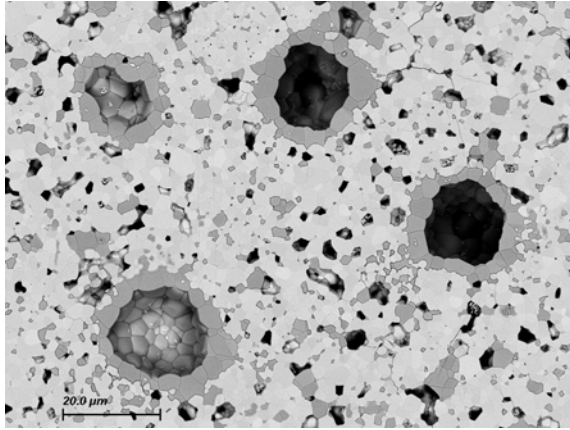
Figure 2: SEM micrography for a composite sample with nominal composition $In_{1.8}Ge_{0.2}O_3$. Sphere-like $In_2Ge_2O_7$ agglomerates (grey phase) can be observed.

All samples exhibit a metallic behavior with the electrical resistivity increasing with temperature except the composite $In_{1.8}Ge_{0.2}O_3$ (not shown). The influence of the germanium fraction on the electrical resistivity at 1000K is shown in figure 3. Starting from undoped In_2O_3 with $\rho \sim 25$ mΩ.cm at 1000K, a very small addition of germanium, of the order 0.1 atom% (x=0.002), leads to a strong decrease of the electrical resistivity, by a factor of 5. Further additions lead to a decrease of the resistivity with a minimum reached at x=0.015 with $\rho \sim 1.5$ mΩ.cm at 1000K. It is noteworthy that this latter value is very close to the best electrical conductivities observed in bulk In_2O_3 based compounds (see for example ref. 12 and ref. therein). Further additions lead to a slow increase of the resistivity. Therefore, we can propose that the solubility limit for Ge in In_2O_3 may be close to x=0.01-0.015 and that there is most probably a doping effect due to the substitution of Ge(+IV) for In(+III) which would lead to an increase of the electrons concentration in the system. The behavior of the thermopower is similar (see Fig. 3). All samples are n-type with the absolute value of the thermopower increasing with temperature (not shown), which is consistent with the metal-like behavior of the electrical resistivity. The influence of the germanium fraction on the thermopower at 1000K is shown in

figure 3. Starting from undoped In_2O_3 with $S \sim -225$ μV.K^{-1} at 1000K, a very small addition of germanium leads to a decrease of the thermopower, which reaches a constant value $S \sim -110$ μV.K^{-1} when the germanium fraction exceeds x=0.015.
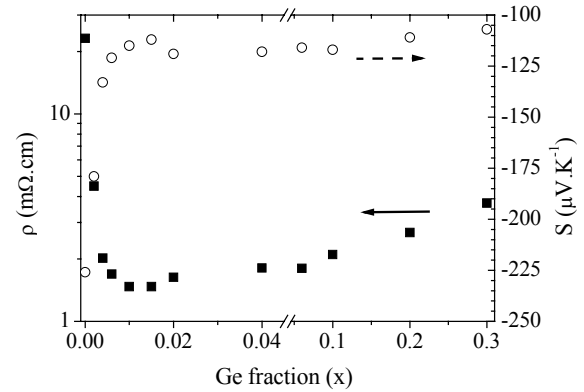

Figure 3: Influence of the germanium fraction on the electrical resistivity (filled symbols) and the thermopower (open symbols) at 1000K. Note the break in the x-coordinate.

Thus, whereas the XRD and SEM studies show that the solubility of germanium in In_2O_3 is very small or even null, the decrease of the electrical resistivity and of the absolute value of the thermopower suggests strongly that small Ge fractions substitute for In leading to an increase of the electrons concentration. Then the increase of the electrical resistivity after the minimum may be connected to the increasing fraction of highly resistive $In_2Ge_2O_7$ phase or to the decreasing density. $In_2Ge_2O_7$ being highly resistive, the presence of inclusions hardly influences the thermopower values that remain constant above the solubility limit. Indeed, it has been shown that small inclusions of a highly resistive phase into a conductive matrix do not influence the magnitude of the thermopower which is mainly linked to the matrix.

This conclusion is confirmed by the Hall effect measurements shown in figure 4. The electrons concentration increases very rapidly from $1.7 \cdot 10^{18}$ cm^{-3} in undoped In_2O_3 to $1.6 \cdot 10^{20}$ cm^{-3} in $In_{1.99}Ge_{0.01}O_3$ and then saturates around $1-2 \cdot 10^{20}$ cm^{-3}. These values are well explained assuming one free

electron for each germanium atom below the solubility limit (dashed line in figure 4).
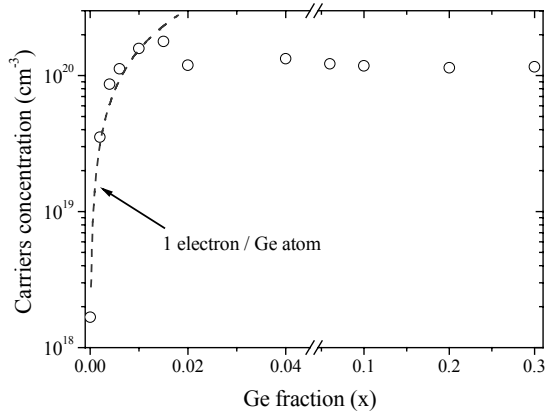

Figure 4: Influence of the germanium fraction on the room-temperature electrons concentration. The line is a simulation assuming one free electron per Ge atom.
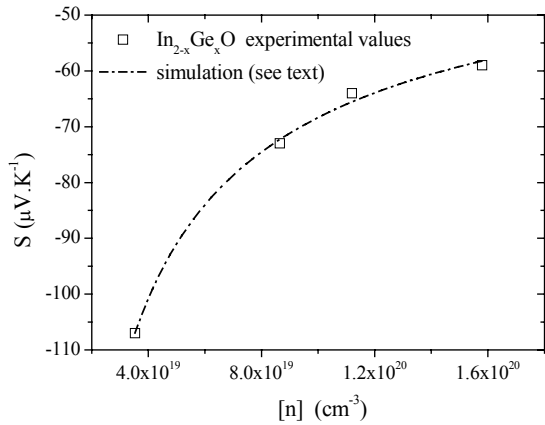

Figure 5: Evolution of the thermopower with the electrons concentration in the single-phase domain at room temperature. The line is a simulation assuming a diffusion thermopower (see text)

Besides this increase of the electrons concentration with germanium doping explains the decrease of the electrical resistivity up to the solubility limit, it also explains the decrease of the thermopower. Figure 5 shows the influence of the electrons concentration on the thermopower below the solubility limit. The decrease of the thermopower can be reasonably well simulated by considering a diffusion model with $S_{diff} \propto m^* T n^{-2/3}$ [13] with n the electrons concentration and m^* the electrons effective mass. A fit of our data assuming this model leads to $m^* = 0.31\ m_e$, which is in very good agreement with the effective

mass determined using optical characterization [14].

Despite the decrease of the thermopower with increasing Ge doping, it appears that this doping is very efficient to enhance the thermoelectric power factor at high temperature (figure 6). Starting from undoped In_2O_3 with PF $\sim 2.2\,10^{-4}$ $W.m^{-1}.K^{-1}$ above 1000K, a very small addition of germanium, of the order x=0.002-0.006, leads to a strong increase of the power factor, by a factor of 4 approximately. Further additions of germanium, higher than x=0.02, lead to a slow decrease of the power factor, which is linked to the increase of the electrical resistivity. However, this decrease could probably be moderated by achieving a better densification of the samples.
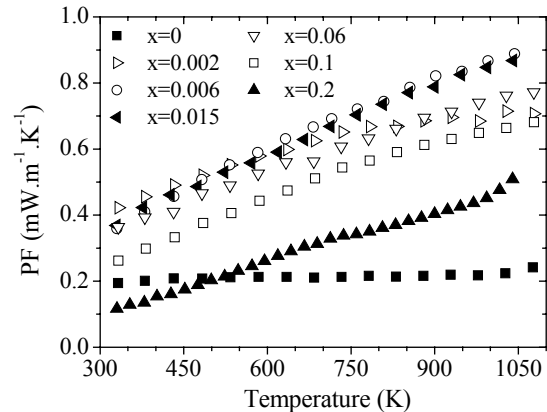

Figure 6: Temperature dependence of the power factor $S^2\sigma$ in the series with nominal composition $In_{2-x}Ge_xO_3$.

Figure 7 shows the influence of the germanium fraction on the thermal conductivity. Whatever the germanium content, the thermal conductivity decreases with increasing temperature as it is exemplified in the inset in the case of Ge = 0.06. At room temperature, the influence of the germanium additions is very important, with λ decreasing from about 10 $W.m^{-1}.K^{-1}$ in undoped In_2O_3 to 3.3 $W.m^{-1}.K^{-1}$ in the composite $In_{1.8}Ge_{0.2}O_3$. This trend is similar at higher temperature although the magnitude of the thermal conductivity decrease is smaller. It is

noteworthy that λ is smaller in highly substituted samples than in the undoped one although the electrical resistivity is smaller too.
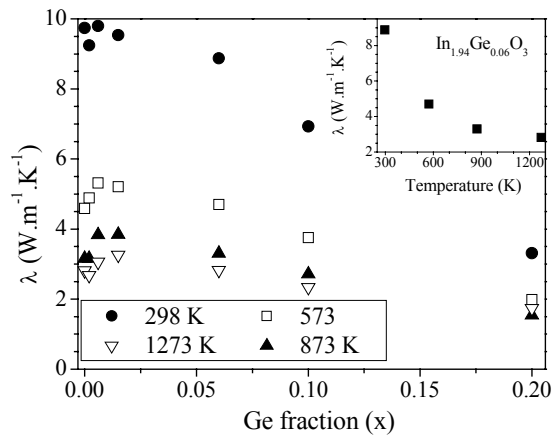

Figure 7: Influence of the germanium fraction on the thermal conductivity in the series with nominal composition $In_{2-x}Ge_xO_3$. Inset: Temperature dependence of the thermal conductivity of the composite $In_{1.94}Ge_{0.06}O_3$.
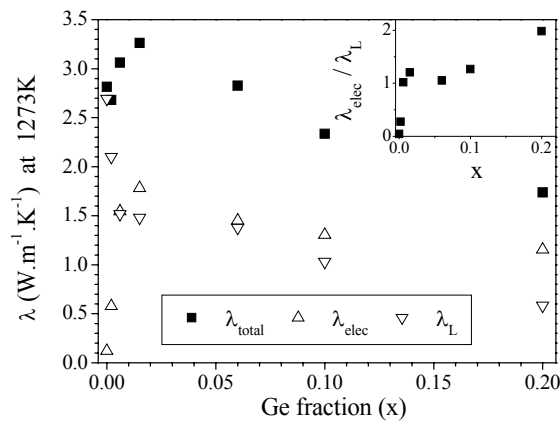

Figure 8: Calculated electronic and lattice part of the thermal conductivity at 1273K as a function of the germanium fraction. The inset shows the ratio of the electronic part to the lattice part of the total thermal conductivity at 1273K as a function of the germanium fraction.

The total thermal conductivity can be divided into two parts, one originating from the charge carriers and linked to the electrical conductivity by the Wiedmann-Franz law, and the other one originating from the heat carrying phonons. Figure 8 shows the calculated electronic and lattice part of the thermal conductivity at 1273K as a function of the germanium fraction. Starting from undoped In_2O_3 where the

main part of the thermal conductivity is due to the phonons, small additions of Ge lead to a strong increase of the electronic part, which is linked to the strong decrease of the electrical resistivity due to germanium doping. Further additions of germanium above the solubility limit lead to a slow decrease of the electronic part due to the slow increase of the electrical resistivity. The lattice part of the thermal conductivity monotically decreases from about $3\ W.m^{-1}.K^{-1}$ in undoped In_2O_3 to about $0.6\ W.m^{-1}.K^{-1}$ in the composite $In_{1.8}Ge_{0.2}O_3$.

The inset of the figure 8 shows the influence of the germanium fraction on the ratio λ_{elec}/λ_L (the higher is this ratio, the higher is the thermoelectric figure of merit ZT). In undoped In_2O_3, the thermal conductivity is dominated by its lattice part. The first increase of λ_{elec}/λ_L for low germanium fractions is mainly linked to the decrease of the electrical resistivity. The ratio exhibits a local maximum for a germanium fraction that corresponds to the solubility limit. However, it is noteworthy that λ_{elec}/λ_L increases when x increases for high germanium fractions, although the electrical conductivity (and therefore λ_{elec}) decreases. It means that the germanium additions are more effective in decreasing the phonons mean free path that the charge carriers mobility and are therefore suitable for improving the thermoelectric efficiency. Nevertheless, as the presence of $In_2Ge_2O_7$ and the increase of porosity due to the crown-like agglomerates formation are strongly linked, it is not possible to determine whether this effect on the thermal conductivity mainly originates from the inclusions or from the pores.

The Ge doping leading to both an increase of the power factor and a decrease of the lattice thermal conductivity, it is very effective in improving the thermoelectric figure of merit ZT. Figure 9 shows the calculated ZT as a function of the germanium fraction in the series with nominal composition $In_{2-x}Ge_xO_3$. ZT increases with the increasing temperature

for all compositions. High temperature ZT outreaches 0.1 in In_2O_3, which is higher than in undoped ZnO [4] and almost one third of the values of the best n-type thermoelectric oxides. The figure of merit is strongly enhanced by Ge additions, with ZT=0.46 at 1273K in the composite compound $In_{1.8}Ge_{0.2}O_3$. This value is higher than that of the best previously reported bulk n-type oxides. Moreover, from the slope of the ZT versus germanium content ZT(x) curve, higher ZT values can reasonably be expected for higher Ge fractions.
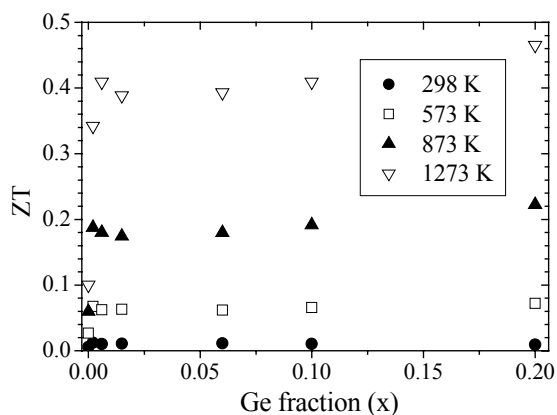

Figure 9: Calculated dimensionless figure of merit ZT as a function of the germanium fraction in the series with nominal composition $In_{2-x}Ge_xO_3$.

CONCLUSION

We have shown that Ge-doped In_2O_3 is a very promising thermoelectric oxide. Although the germanium solubility limit is very small, there is a large increase of the electrons concentration with Ge doping. It leads to a strong decrease of the electrical resistivity, which becomes metal-like, and a moderate decrease of the thermopower, which is well explained using a diffusion term. Therefore, high power factors are observed, close to 1 $mW.m^{-1}.K^{-1}$ around 1100K. As the thermal conductivity of undoped In_2O_3 is small at high temperature, the dimensionless figure of merit ZT is quite high, reaching 0.1. Moreover, further Ge additions, leading to the presence of $In_2Ge_2O_7$ agglomerated inclusions, appear to be very effective in decreasing the lattice

thermal conductivity, with λ being lower than 2 $W.m^{-1}.K^{-1}$ in the composite $In_{1.8}Ge_{0.2}O_3$ at high temperature. This low thermal conductivity, coupled with high power factors, leads to very promising thermoelectric figures of merit with ZT > 0.45 in the composite $In_{1.8}Ge_{0.2}O_3$ at 1273 K. This high values make these materials suitable for high temperature energy conversion in oxide thermoelectric modules.

REFERENCES

[1] *Recent Trends in thermoelectric materials research I-III*, in: T.M. Tritt (Ed.), Semiconductors and Semimetals, vol 69-71, Academic, San Diego, USA, 2000.
[2] G.D. Mahan *et al.*, Phys. Today **50**, 42 (1997)
[3] B.T. Cong *et al.*, Physica B **352**, 18 (2004)
[4] M. Ohtaki *et al.*, J. Appl. Phys. **79**, 1816 (1996)
[5] H. Kaga *et al.*, Jpn J. Appl. Phys. **43**, 7133 (2004)
[6] K.L. Chopra *et al.*, Thin Solid Films **102**, 1 (1983)
[7] D. Bérardan *et al.*, Solid State Comm. **146**, 97 (2008)
[8] J. Rodriguez-Carvajal, Physica B **192**, 55 (1993)
[9] M. Marezio, Acta Cryst. **20**, 723 (1966)
[10] R.D. Shannon *et al.*, J. Solid State Chem. **2**, 199 (1970)
[11] R.D. Shannon, Acta Cryst. A **32**, 751 (1976)
[12] L. Bizo *et al.*, Solid State Comm. **136**, 163 (2005)
[13] *The Theory of Metals*, A.H. Wilson, Cambrigde University Press (1965).
[14] Z.M. Jarzebski, Phys. Status Solidi A **71**, 13 (1982)